Empirical Evaluation of Four Microwave Radiative Forward Models Based on Ground-Based Radiometer Data Near 20 and 30 GHz

C. Cimini
Centre of Excellence on Atmospheric Modeling and Remote Sensing
University of L'Aquila
L'Aquila, Italy
and
Science and Technology Corporation
Hampton, Virginia

E. R. Westwater
Cooperative Institute for Research in Environmental Sciences
University of Colorado
National Oceanic and Atmospheric Administration
Environmental Technology Laboratory
Boulder, Colorado

S. J. Keihm
National Aeronautics and Space Administration
Jet Propulsion Laboratory
California Institute of Technology
Pasadena, California

Y. Han
National Oceanic and Atmospheric Administration
National Environmental Satellite Data and Information Service
Office of Research and Application
Camp Springs, Maryland

F. S. Marzano and P. Ciotti
Electrical Engineering Department
University of L'Aquila
L'Aquila, Italy

Introduction

Recent experiments have shown excellent calibration accuracy for ground-based microwave radiometers. On the other hand, uncertainty related to the radiative properties of the atmosphere is the main limiting factor for the retrieval of atmospheric water vapor. In this work we intend to study the differences in brightness temperature (Tb) as computed using a variety of four among the most used microwave absorption models. Furthermore, we want to compare theoretical prediction with empirical data, in order to evaluate the ability of each model to reproduce the actual behavior of the atmosphere. The four models we consider are hereafter referred as LIEBE87 (Liebe and Layton 1987), LIEBE93 (Liebe et al. 1993), ROSEN98 (Rosenkranz 1998) and MONORTM (Delamere et al. 2002, Cady-Pereira et al. 2002). By processing three readily available historical datasets of radiosonde observations with these models, we computed the main Tb for each model in three contrasting environments: tropical, mid and arctic latitudes. Then, we discuss the differences in computed Tb between the four models. We focus on the spectral range from 20 to 30 GHz, which is commonly used for ground-based estimates of atmospheric water vapor by microwave radiometers, and so routinely measurements are often available. Empirical data were collected during the water vapor intensive operational period (WVIOP), held in September/October 2000 at the Atmospheric Radiation Measurement (ARM) program's Southern Great Plains (SGP) site, in Lamont, Oklahoma. Three microwave radiometer (MWR) units were deployed, with a total of seven channels from 20.6 to 31.65 GHz. Other than radiometric observations, during the

WVIOP2000 there were three-hourly radiosonde launches, deploying two different kinds of sensors, the RS80 and RS90. Since RS90 are believed to reduce the "dry-bias" affecting the RS80 (Lesht 1999), the WVIOP2000 provided a unique opportunity of having high quality atmospheric profiles and ground-based observations (Cimini et al. 2003). Thus, we show the comparison of Tb computed from RS90 measurements using the four models with Tb observations from the MWR units, and discuss a possible choice between the considered models.

Datasets and Simulations

From three historical datasets of arctic (5141), mid-latitude (12670), and tropical (1086) radiosondes, we have computed down-welling brightness temperature in the frequency range around the water vapor line at 22 GHz, using a variety of four radiative forward models (FM). The precipitable water vapor (PWV) ranges from 0.05 to 3.5 cm with a mean value of 0.7 cm for the arctic dataset, from 0.2 to 6.0 with 2.1 cm mean at mid-latitudes, while between 2.3 and 7.0 cm with mean 5.0 cm for the tropics dataset. From the simulated Tb spectra (19 to 26 GHz, 0.1 GHz spectral resolution), we have extracted the mean Tb spectrum within this range, for each model and for each environment. In Figure 1, we show the mean value of simulated Tb for each model as obtained from the three datasets (a: arctic; b: mid-latitudes; c: tropics). It is evident that the four models act in a similar way in the three environments: LIEBE87 and ROSEN98 tend to be very close, while LIEBE93 shows a warmer bias (about 1 K in the arctic, up to 3 K in the tropics). On the other hand, MONORTM shows a different behavior: it tends to be close to LIEBE93 up to 23 GHz, while it becomes very close to LIEBE87 and ROSEN98 at higher frequencies.

In order to understand better how the models differ, we show, for each environment (Figure 2), the differences between mean Tb from each model and from the LIEBE87, taken as a reference. In the (a) arctic, with very low amounts of PWV, LIEBE87 shows to be colder than every other model for the whole range. We see almost the same situation for the (b) mid-latitudes, at medium values of PWV, but ROSEN98 shows to be the coldest for frequencies very close to the center of the line. In the (c) tropics, at higher values of water vapor, LIEBE93 is still warmer than every other model, while ROSEN98 and MONORTM show a trend that depends on frequency with respect to LIEBE87. ROSEN98 is colder close to the center of the line, while it is warmer along the wings. MONORTM is warmer below 23.8 GHz and colder for higher frequencies. Note that at 23.8 GHz, which is the central frequency used by ARM operational radiometers, LIEBE87, ROSEN98, and MONORTM are all pretty close (differences less than 0.5 K).

Microwave Radiometers and Radiosondes

During the WVIOP2000 we had several MWR units running continuously for about a month. All of them were continuously scanning in the east-west direction, so we applied the tip curve method to refine calibration (Han and Westwater 2000). From this set of instruments, we selected for this work the three units that gave best performances (Cimini et al. 2003). These units are the ARM dual channel Central Facility (23.8, 31.4 GHz), the National Aeronautic Space Administration Jet Propulsion Laboratory three-channel radiometer (20.7, 22.2, 31.4 GHz), and the National Oceanic and Atmospheric Administration/Environmental Technology Laboratory dual channel circulating scanning radiometer

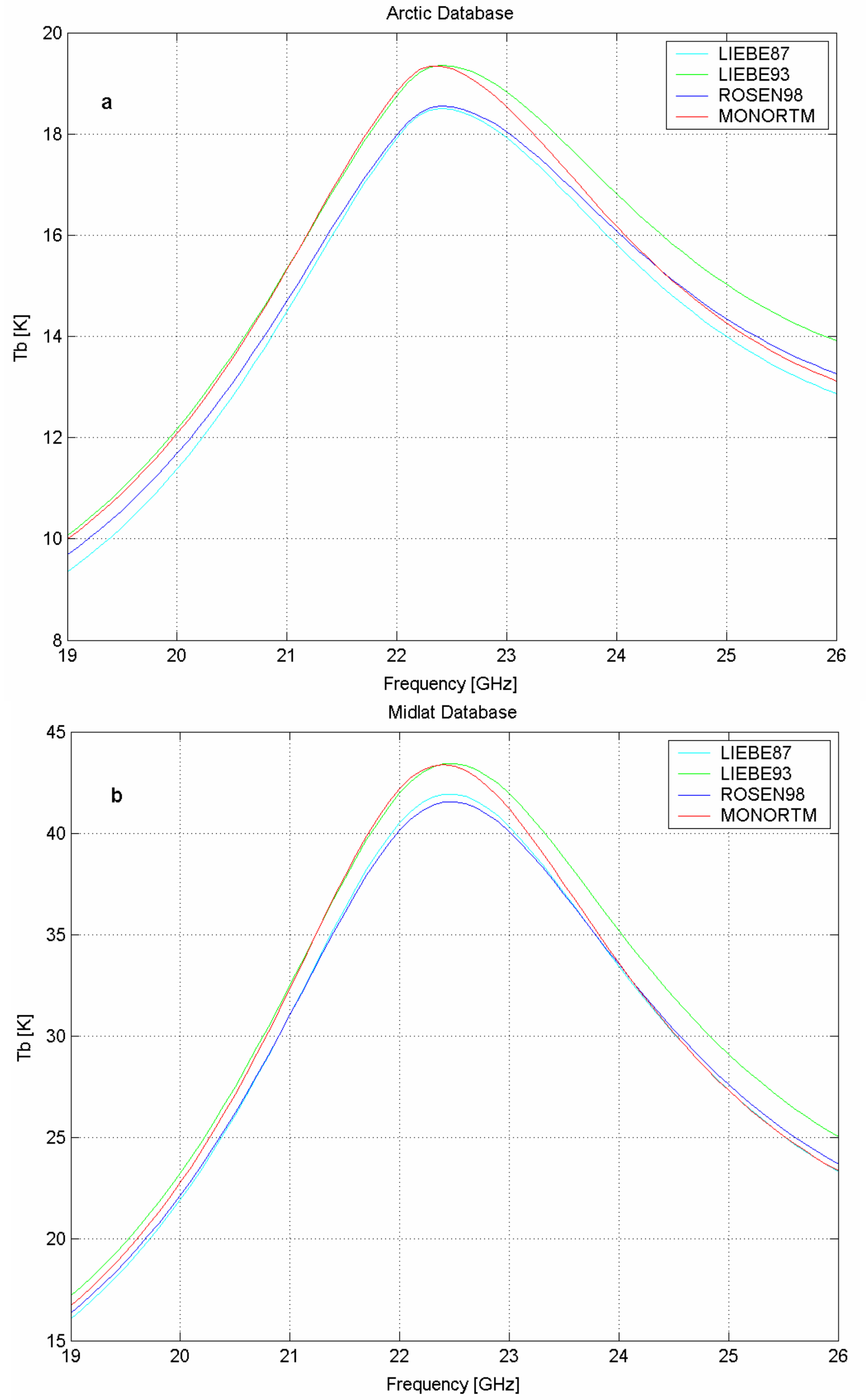

Figure 1. Mean Tb computed using the four absorption models from the (a) arctic, (b) mid-latitude, and (c) tropic radiosonde database.

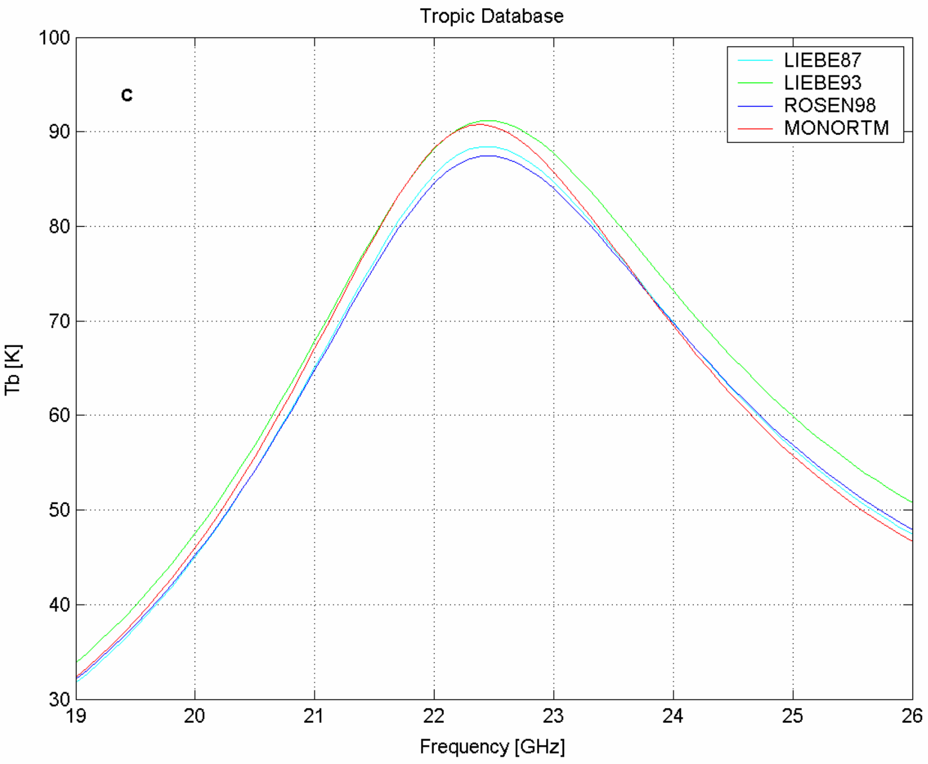

Figure 1. (contd)

(20.6, 31.65 GHz), hereafter referred as ACF, JPL, and CSR, respectively. These radiometers have shown a calibration accuracy of the order of 0.5 K (Cimini et al. 2003). In addition, there were three-hourly radiosonde launches, deploying two different kinds of sensors, the usual RS80 and the new generation RS90. Since RS90 are believed to reduce the “dry-bias” affecting the RS80 (Lesht 1999), the WVIOP2000 provided a unique opportunity of having high quality atmospheric profiles and ground-based observations.

In Figure 3, we show the Tb spectrum from 20 to 32 GHz computed using the four absorption models (solid lines) from tropospheric profiles of pressure, humidity and temperature measured by a RS90 radiosonde (2000/10/01 05:28:00 Universal Time Coordinates [UTC]), and ground-based observations from the three MWR units (squares for CSR, triangles for JPL, circles for ACF). By comparing the four lines, we notice some of the features we discussed earlier, plus some more for higher frequency. This figure shows just one case, so we cannot take a conclusion basing on it, but it shows the frequency distribution of the instruments’ channels. Then, taking the whole set of radiosondes launched during the WVIOP2000 (288), but considering only the RS90 (55), and screening out measurements in cloudy conditions, we end up with a set of 34 atmospheric profiles. For each of these profiles, we computed the synthetic Tb with the four absorption models, at every frequency covered by the instruments’ channels, in order to compare simulations with empirical observations. In Figure 4 we show the scatter plots between MWR observations (Tb(MWR), X axis) and simulations from the RS90 using the four FM (Tb(RS90/FM), Y axis). We show the following channels: (a) CSR 20.6 GHz, (b) JPL 20.7 GHz, (c) JPL 22.2 GHz, (d) ACF 23.8 GHz, (e) ACF 31.4 GHz, and (f) CSR 31.65 GHz.

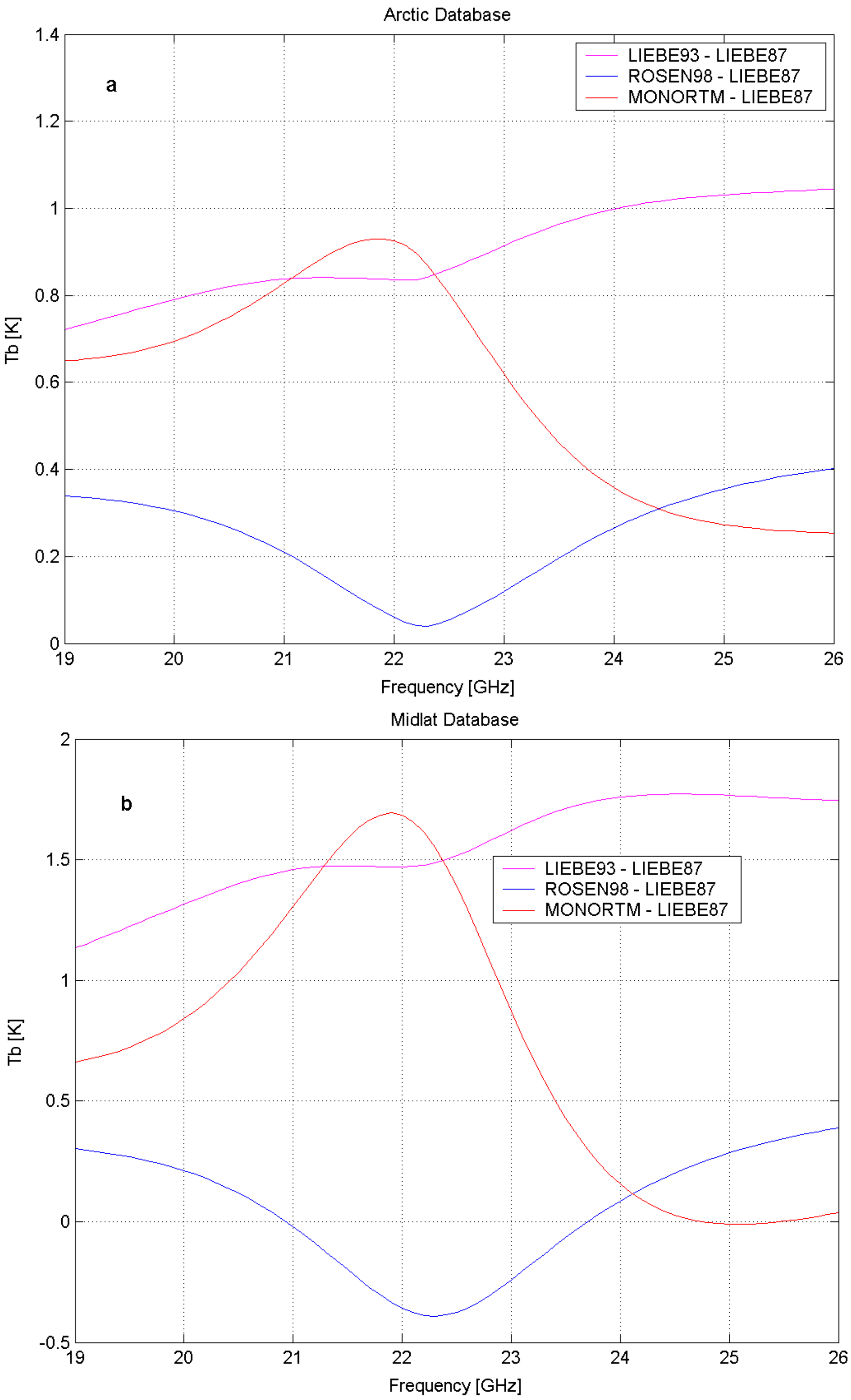

Figure 2. Differences between Tb computed using three absorption models (LIEBE93, ROSEN98, and MONORTM) with respect to Tb computed using LIEBE87, for the (a) arctic, (b) mid-latitude, and (c) tropic radiosonde database.

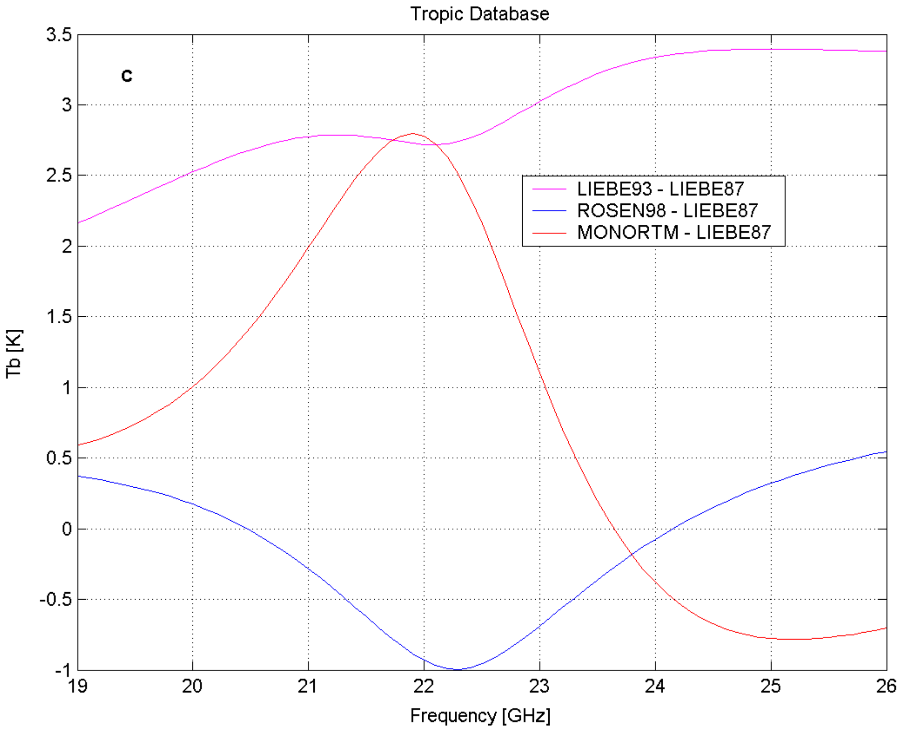

Figure 2. (contd)

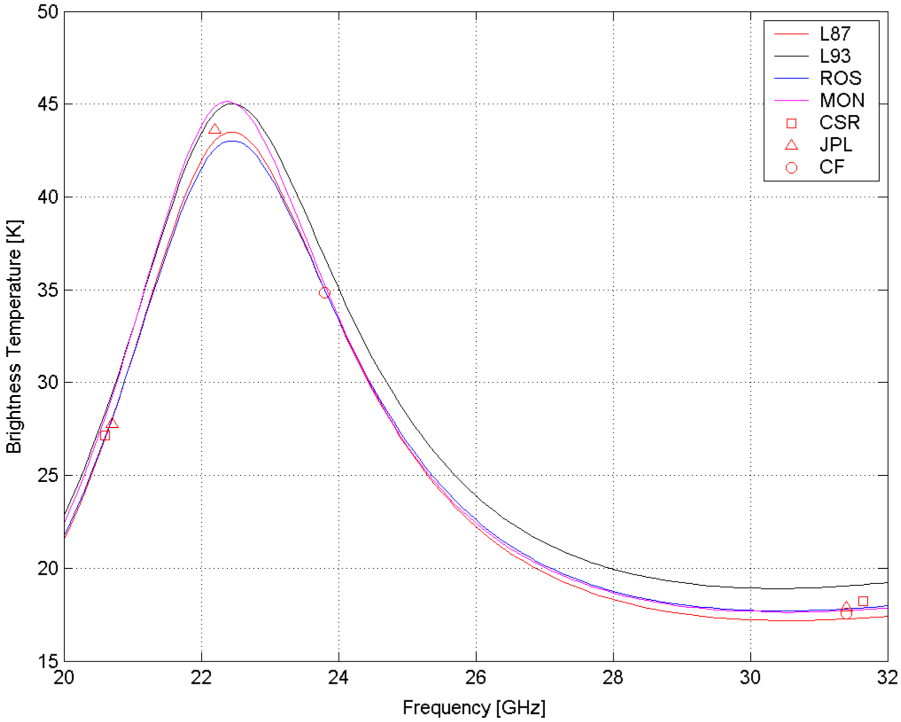

Figure 3. Ground-based Tb observations from three MWR units (CSR, JPL, ACF) and simulations computed using four absorption models (solid lines) from pressure, humidity, and temperature profiles measured by a RS90 radiosonde (2000/10/01 05:28:00 UTC).

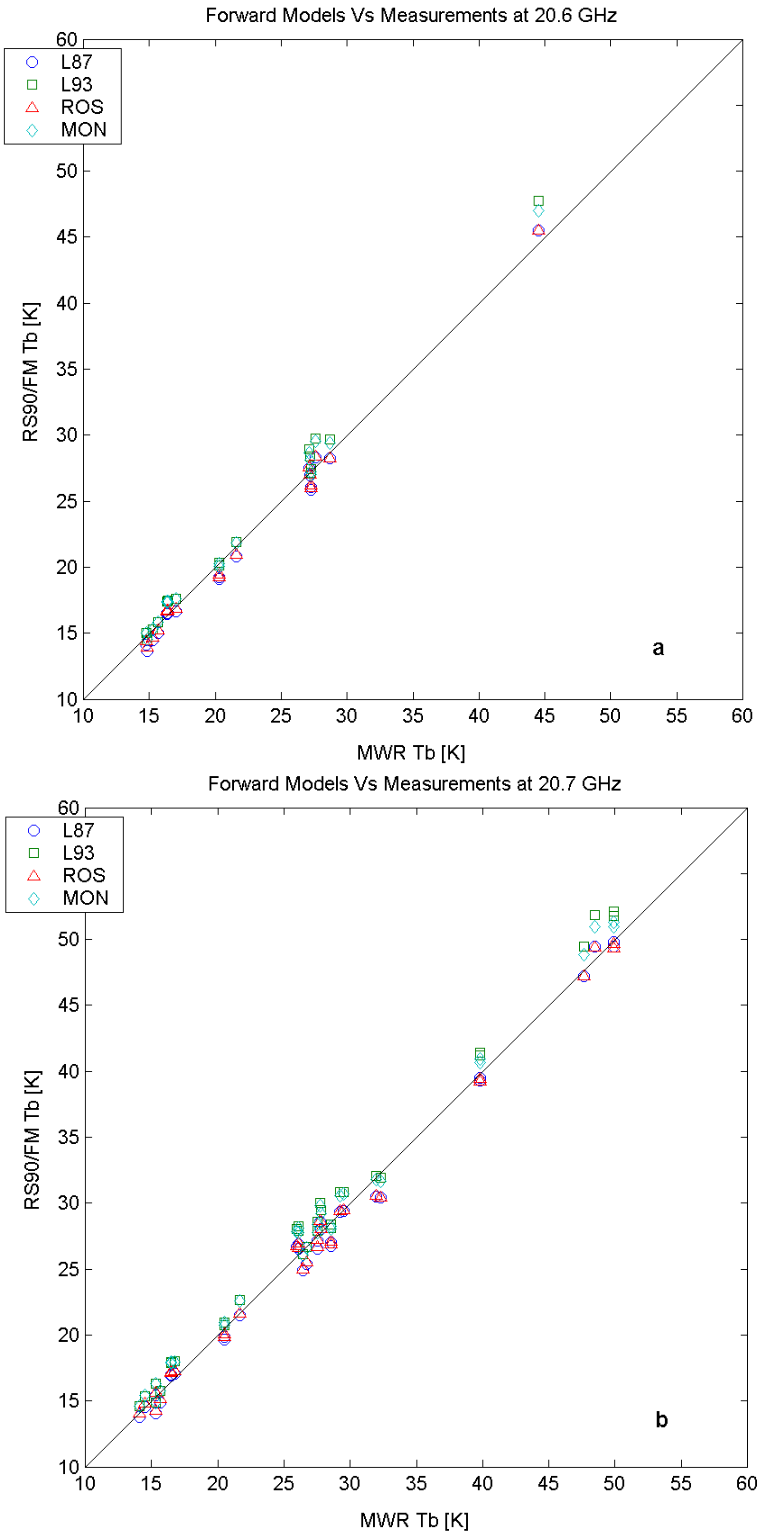

Figure 4. Scatter plot between brightness temperature as observed by microwave radiometers (Tb[MWR]) and computed from RS90 measurements using four absorption models (Tb[RS90/FM]). Each subplot corresponds to a different channel: (a) CSR 20.6 GHz, (b) JPL 20.7 GHz, (c) JPL 22.2 GHz, (d) ACF 23.8 GHz, (e) ACF 31.4 GHz, and (f) CSR 31.65 GHz.

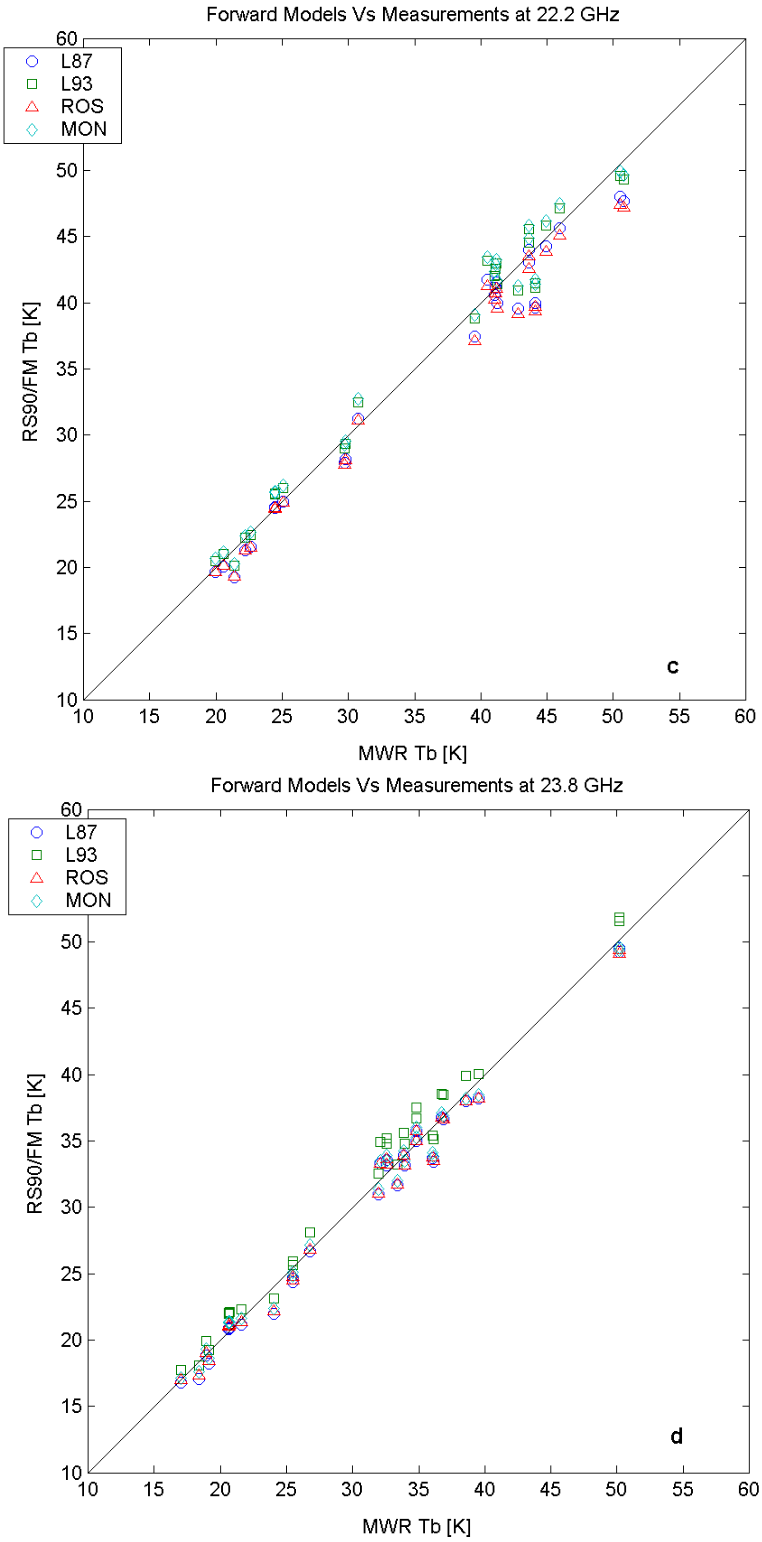

Figure 4. (contd)

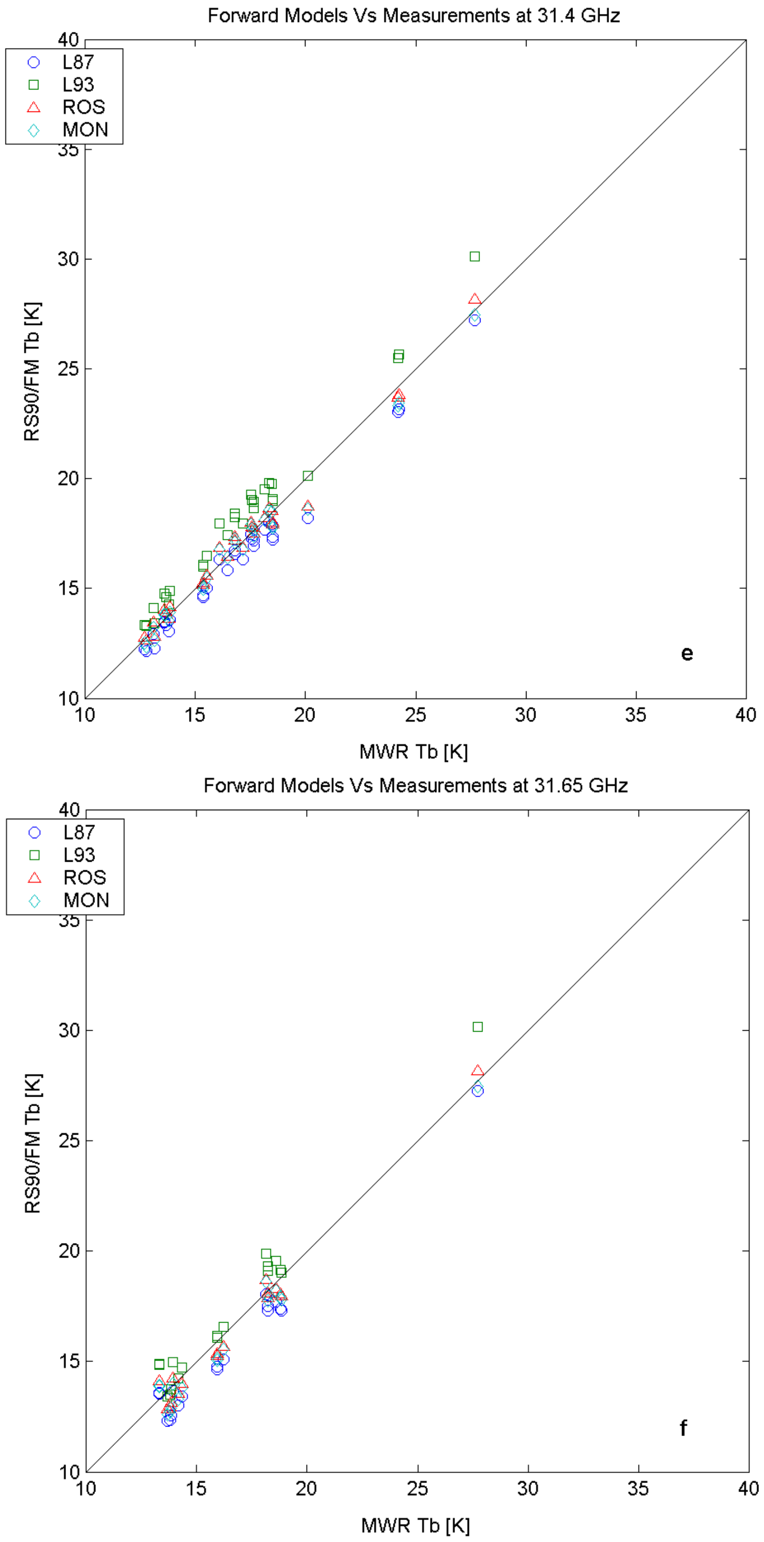

Figure 4. (contd)

Note that sample size is not constant for all the plots, because radiometers were running independently, and so experienced acquisition gaps (due to system crashes or voluntary shut-downs) at different time. Mean value (BIAS) and standard deviation (STDV) of the difference between observations and simulations ($\Delta Tb = Tb(MWR)-Tb(RS90/FM)$ at each frequency have been grouped in Figure 5. Note that in this figure has been added the JPL 31.4 GHz channel, which was not shown among the scatter plots. It might be disappointing to see quite different results from two equivalent channels (31.4 GHz for JPL and ACF in Figure 5a), but we have to remind that the MWR measurements are not always coexistent, and due to the relatively poor sample of radiosondes (34), the statistics is sensitive to that.

Summary and Comments

We have shown that differences in the 19 to 26 GHz range between Tb simulations based on four different microwave absorption models are of the order of 1 K in the arctic environment (0.7 cm mean PWV), of 2 K at mid-latitudes (2.1 cm mean PWV) and up to 4 K in the tropical regions (5.0 cm mean PWV). This sort of differences leads to an uncertainty in PWV estimates by microwave radiometry of the order of few millimetres. Thus, presently, absorption model uncertainties are the main limiting factor to the retrieval of PWV from MWR (Keihm et al. 2002).

From the comparison of simulation with observations, we have seen that the STDV of Tb(MWR)-Tb(RS90/FM) gives similar results for the four models, with the scatter increasing near the center of the water vapor line (Figure 5b). For what concern the mean value of the differences between simulations and observations (Figure 5a), we can note the following:

1. LIEBE87 gives a positive BIAS (simulations colder than measurements)
    a. less than 0.5 K for hinge point channels (20.6-20.7-23.8 GHz, see [Cimini, this proceedings])
    b. of about 1 K at the center of the line (22.2 GHz)
    c. between 0.5 and 1 K for the window channels (31.4-31.65 GHz)
2. LIEBE93 gives a negative BIAS (simulations warmer than measurements)
    a. between 0.5 and 1 K for every channel but 22.2 GHz, where it is less than 0.5 K
3. ROSEN98 gives a positive BIAS
    a. smaller than 0.6 for every channel but 22.2 GHz, where it reaches 1.5 K.
4. MONORTM gives a BIAS
    a. between 0.5 and 1 K for frequency up to 22.2 GHz
    b. less than 0.4 K for higher frequency (except the JPL 31.4 GHz)

Thus, according to our results, we can conclude that there is not a unique forward model, among the ones we considered, which represents best the empirical data in the whole spectral range. Indeed, the ROSEN98 gives best results for frequency around the first hinge point (20.6 to 20.7 GHz), the LIEBE93 and the MONORTM are preferable for frequency close to the center of the line (22.2 GHz) while the MONORTM for the second hinge point (23.8 GHz), while once again the ROSEN98 for window channels (31.4 to 31.65 GHz). This means the question about which model agrees best with observations is still open, but also that it might be not enough to consider just one or two channels.

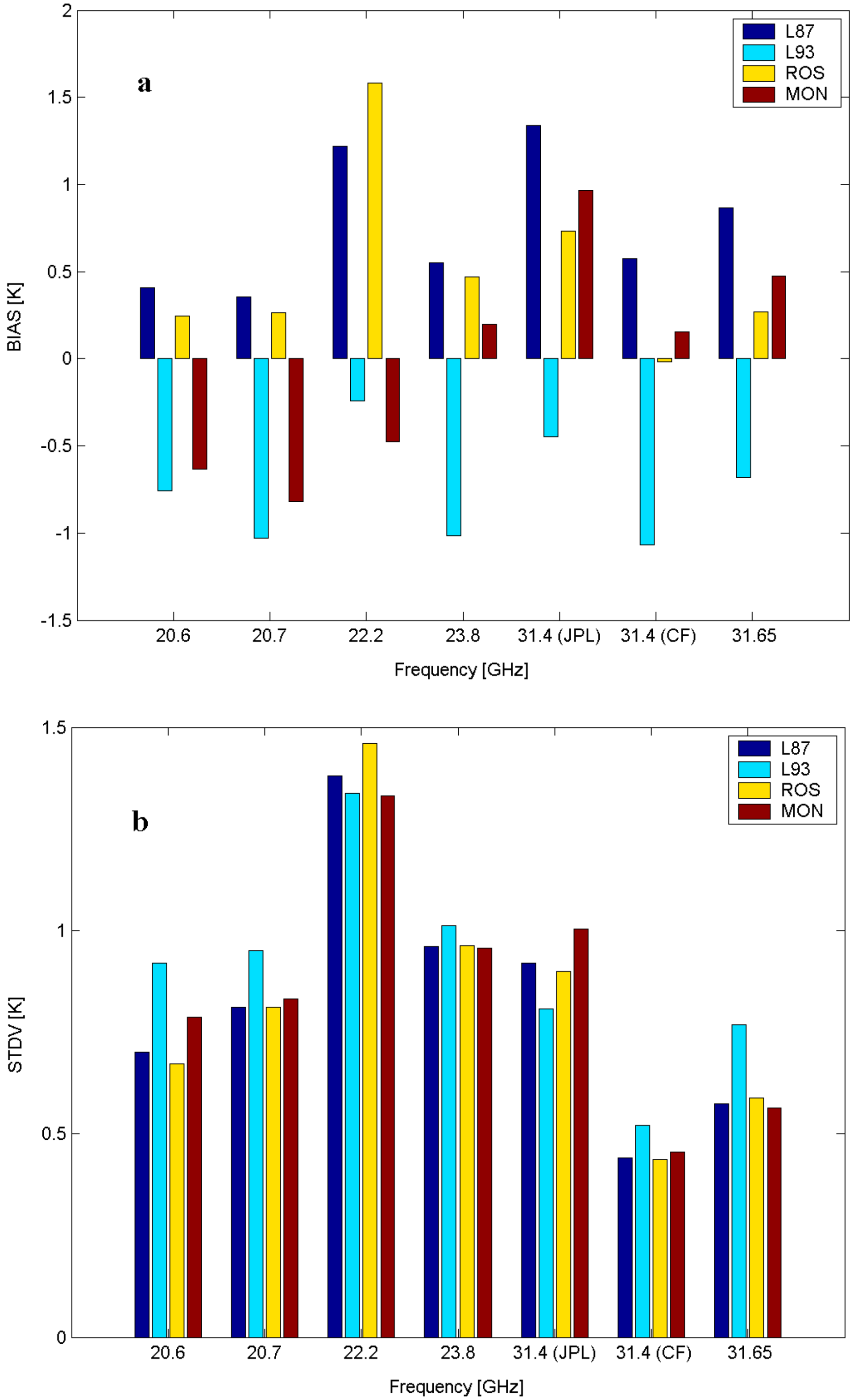

Figure 5. (BIAS, a) mean value and (STDV, b) standard deviation of ΔTb = Tb(MWR)-Tb(RS90/FM) for each frequency available during the WVIOP2000.

Future Developments

For our future research, we are focusing on three major developments of this work. First of all, we intend to include other FM in the set under study, in order to cover as much as possible the variety available in literature. For instance, there are two other models, which are discussed in (Keihm et al. 2002) that we are currently implementing. Moreover, it would be useful to increase the radiosonde sample size. This can be done by extending our study to a time period longer than the WVIOP2000, although this would reduce the set of MWRs available. Nevertheless, a multi-channel MWR is working at the ARM SGP site since more than one year, providing a powerful source for future comparisons. Another piece of information would come from considering RS90 measurements and MWR observations in different environments, such the arctic and the tropics. This development is already ongoing, using data from the ARM NSA and TWP sites. Unless particular experiments (Westwater et al. 2001), in this study we are unfortunately limited to only one dual channel radiometer.

Acknowledgements

The work presented in this paper was sponsored by the Environmental Science Division of the Department of Energy as a part of their Atmospheric Radiation Program and by Science and Technology Corporation (STC Contract No. 45-EANA-0-00055).

Corresponding Author

,

References

Cady-Pereira, K., S. A. Clough, S. Boukabara, J. C. Liljegren, 2002: The physical retrieval of PWV and CLW with MonoRTM using ARM MWR Data. , Proc. of 12th ARM Science Team Meeting, 2002.

Cimini, D., E. R. Westwater, Y. Han, and S. Kehim, 2003: Ground-based microwave radiometer measurements and radiosonde comparisons during the WVIOP2000 field experiment. *TGARS*, submitted.

Cimini, D., E. R. Westwater, and Y. Han, 2003: Theoretical analysis of the frequency allocation of the hinge points around 22.235 GHz. This Proceedings.

Delamere J. S., S. A. Clough, E. J. Mlawer, S. Boukabara, K. Cady-Peirera, and M. Shepard, 2002: An update on radiative transfer model development at Atmospheric and Environmental Research, Inc. In *Proceedings of the Twelfth Atmospheric Radiation Measurement (ARM) Science Team Meeting*, ARM-CONF-2002. U.S. Department of Energy, Washington, D.C. Available URL: http://www.arm.gov/docs/documents/technical/conf_0204/delamere-js.pdf

Han, Y., and E. R. Westwater, 2000: Analysis and improvement of tipping calibration for ground-based microwave radiometers. *Trans. Geosci. Rem. Sens.*, **38**(3), 1260-1276.

Keihm S. J., Y. Bar-Sever, and J. C. Liljegren, 2002: WVR-GPS Comparison measurements and calibration of the 20-32 GHz tropospheric water vapor absorption model. *IEEE Trans. Geosci. Remote Sensing*, **40**(6), 1199-1210.

Lesht, B. M., 1999: Reanalysis of radiosonde data from the 1996 and 1997 water vapor intensive observation periods: Application of the Vaisala RS-80H contamination correction algorithm to dual-sonde soundings. In *Proceedings of the Ninth Atmospheric Radiation Measurement (ARM) Science Team Meeting,* U.S. Department of Energy, Washington, D.C. Available URL: http://www.arm.gov/docs/documents/technical/conf_9903/lesht-99.pdf

Liebe, H. J., and D. H. Layton, 1987: Millimeter wave properties of the atmosphere: Laboratory Studies and Propagation Modeling. NTIA Report 87-24, p. 74.

Liebe, H. J., G. A. Hufford, and M. G. Cotton, 1993: Propagation modeling of moist air and suspended water/ice particles at frequencies below 1000. *AGARD Conf. Proc*. 542, pp. 3.1 to 3.10.

Rosenkranz, P. W., 1998: Water vapor microwave continuum absorption: A comparison of measurements and models. *Radio Sciences*, **33**(4), 919-928.

Westwater E. R., P. E. Racette, and D. Cimini, 2001: The Artic Winter Millimeter-Wave Radiometric Experiment: Summary, Conclusion and Recommendations. In *Proceedings of the Eleventh Atmospheric Radiation Measurement (ARM) Science Team Meeting*, ARM-CONF-2001.
U.S. Department of Energy, Washington, D.C. Available URL:
http://www.arm.gov/docs/documents/technical/conf_0103/westwater-er.pdf